Electronic Supplementary Material (ESI) for RSC Advances.

Support Information for:

White-Light Emitting Materials with Tunable Luminescence based on Steady Eu (III) doping Tb (III) Metal-Organic Frameworks

Jingjuan Liu, Wei Sun, Zhiliang Liu*

College of Chemistry and Chemical Engineering, Key Lab of Nanoscience and Nanotechnology, Inner Mongolia University, Hohhot, 010021, P. R. China *Corresponding author.

Fax: +86-471-4994375 Tel: +86-471- 4994375

E-mail addresses: cezlliu@imu.edu.cn (Z. L. Liu)

Content

Table S1. Crystal data and structure refinement for **2**.

	Eu-MOF
Empirical formula	$C_{56}H_{30}Eu_2N_4O_{16}$
Formula weight	1318.76
Temperature(K)	293(2)
Wavelength(Å)	1.54178
Crystal system	Triclinic
Space group	*P*–1
a/Å	11.6136(6)
b/Å	13.4816(8)
c/Å	16.2810(11)
α/(°)	89.934(5)
β/(°)	78.409(5)
γ/(°)	71.845(5)
Volume/Å^3	2367.6(2)
Z	2
Calculated density/ Mg/m^3	1.850
Absorption coefficient/ mm^{-1}	19.480
F(000)	1296
Crystal size/ mm^3	0.09 x 0.08 x 0.08
Theta range for data collection/°	2.78 – 67.02
Limiting indices	-13 ≤ h ≤ 13
	-15 ≤ k ≤ 16
	-19 ≤ l ≤ 14
Reflections collected / unique	14745 / 8435 [R(int) = 0.0927]
Completeness to theta = 67.02	99.8 %
Absorption correction	Semi-empirical from equivalents
Max. and min. transmission	0.3048 and 0.2731
Refinement method	Full-matrix least-squares on F^2
Data / restraints / parameters	8435 / 12 / 704
Goodness-of-fit on F^2	1.029
Final R indices [I>2σ(I)]	R1 = 0.0743, wR2 = 0.1696
R indices (all data)	R1 = 0.1036, wR2 = 0.1981
Largest diff. peak and hole/ e.A^{-3}	1.956 and -1.413

Table S2. Bond lengths [A] and angles [°] for **2**.

Bond lengths [A]			
Eu(1)–O(6)	2.368(7)	Eu(2)–O(2)	2.515(8)
Eu(1)–O(5)A	2.389(7)	Eu(2)–O(3)C	2.533(9)
Eu(1)–O(10)	2.429(8)	Eu(2)–N(4)	2.580(9)
Eu(1)–O(11)A	2.482(7)	Eu(2)–N(3)	2.603(11)
Eu(1)–O(12)A	2.507(8)	Eu(2)–Eu(2)C	3.9580(12)
Eu(1)–N(1)	2.537(8)	O(2)–Eu(2)C	2.366(7)
Eu(1)–N(2)	2.581(8)	O(3)–Eu(2)C	2.533(9)
Eu(1)–O(9)	2.654(9)	O(4)–Eu(2)C	2.455(8)
Eu(1)–Eu(1)A	3.8740(11)	O(5)–Eu(1)A	2.389(7)
Eu(2)–O(2)C	2.366(7)	O(11)–Eu(1)A	2.482(7)
Eu(2)–O(13)B	2.420(8)	O(12)–Eu(1)A	2.507(8)
Eu(2)–O(14)D	2.429(7)	O(13)–Eu(2)E	2.420(8)
Eu(2)–O(4)C	2.455(8)	O(14)–Eu(2)D	2.429(7)
Eu(2)–O(1)	2.467(8)		
Angles [°]			
O(6)–Eu(1)–O(5)A	139.4(3)	O(4)C–Eu(2)–O(3)C	51.7(3)
O(6)–Eu(1)–O(10)	122.6(3)	O(1)–Eu(2)–O(3)C	148.3(3)
O(5)A–Eu(1)–O(10)	74.2(3)	O(2)–Eu(2)–O(3)C	132.2(3)
O(6)–Eu(1)–O(11)A	71.3(2)	O(2)C–Eu(2)–N(4)	140.8(3)
O(5)A–Eu(1)–O(11)A	74.0(3)	O(13)B–Eu(2)–N(4)	140.2(3)
O(10)–Eu(1)–O(11)A	139.3(3)	O(14)D–Eu(2)–N(4)	79.2(3)
O(6)–Eu(1)–O(12)A	78.3(3)	O(4)C–Eu(2)–N(4)	97.4(3)
O(5)A–Eu(1)–O(12)A	96.3(3)	O(1)–Eu(2)–N(4)	80.5(3)
O(10)–Eu(1)–O(12)A	157.0(3)	O(2)–Eu(2)–N(4)	125.0(3)
O(11)A–Eu(1)–O(12)A	51.8(2)	O(3)C–Eu(2)–N(4)	74.7(3)
O(6)–Eu(1)–N(1)	83.2(2)	O(2)C–Eu(2)–N(3)	144.6(3)
O(5)A–Eu(1)–N(1)	136.9(3)	O(13)B–Eu(2)–N(3)	76.7(3)
O(10)–Eu(1)–N(1)	88.1(3)	O(14)D–Eu(2)–N(3)	139.4(3)
O(11)A–Eu(1)–N(1)	132.7(2)	N(4)–Eu(2)–N(3)	63.6(3)
O(12)A–Eu(1)–N(1)	84.9(3)	O(2)C–Eu(2)–O(13)B	75.8(3)
O(6)–Eu(1)–N(2)	137.4(3)	O(2)C–Eu(2)–O(14)D	75.5(2)
O(5)A–Eu(1)–N(2)	75.3(3)	O(13)B–Eu(2)–O(14)D	137.3(2)
O(10)–Eu(1)–N(2)	84.5(3)	O(2)C–Eu(2)–O(4)C	73.9(3)
O(11)A–Eu(1)–N(2)	111.0(3)	O(13)B–Eu(2)–O(4)C	75.4(3)
O(12)A–Eu(1)–N(2)	72.7(3)	O(14)D–Eu(2)–O(4)C	124.7(3)
N(1)–Eu(1)–N(2)	64.0(3)	O(2)C–Eu(2)–O(1)	123.8(2)

O(6)–Eu(1)–O(9)	73.3(3)	O(13)B–Eu(2)–O(1)	89.1(3)
O(5)A–Eu(1)–O(9)	120.0(3)	O(14)D–Eu(2)–O(1)	81.4(3)
O(10)–Eu(1)–O(9)	50.7(3)	O(4)C–Eu(2)–O(1)	153.3(3)
O(11)A–Eu(1)–O(9)	133.6(3)	O(2)C–Eu(2)–O(2)	71.6(3)
O(12)A–Eu(1)–O(9)	143.7(3)	O(13)B–Eu(2)–O(2)	72.7(3)
N(1)–Eu(1)–O(9)	69.8(3)	O(14)D–Eu(2)–O(2)	68.6(2)
N(2)–Eu(1)–O(9)	115.3(3)	O(4)C–Eu(2)–O(2)	137.6(3)
O(4)C–Eu(2)–N(3)	77.9(3)	O(1)–Eu(2)–O(2)	52.2(2)
O(1)–Eu(2)–N(3)	77.4(3)	O(2)C–Eu(2)–O(3)C	70.1(3)
O(2)–Eu(2)–N(3)	120.0(3)	O(13)B–Eu(2)–O(3)C	122.6(3)
O(3)C–Eu(2)–N(3)	107.8(3)	O(14)D–Eu(2)–O(3)C	74.9(3)

Symmetry transformations used to generate equivalent atoms:

A: –x, –y+2, –z+2 B: x, y–1, z C: –x, –y+1, –z+1 D: –x, –y+2, –z+1 E: x, y+1, z

Table S3. The initial molar radio and real content measured by ICP for compounds **3–6**.

Compound	Initial molar radio	ICP	
		Tb	Eu
3	1:59	1.83	98.17
4	1:39	2.80	97.20
5	1:29	3.46	96.54
6	1:19	5.61	94.39

Figure S1. The excitation and emission spectroscopy for free H_4btca ligand(a), phen ligand(b).

a b

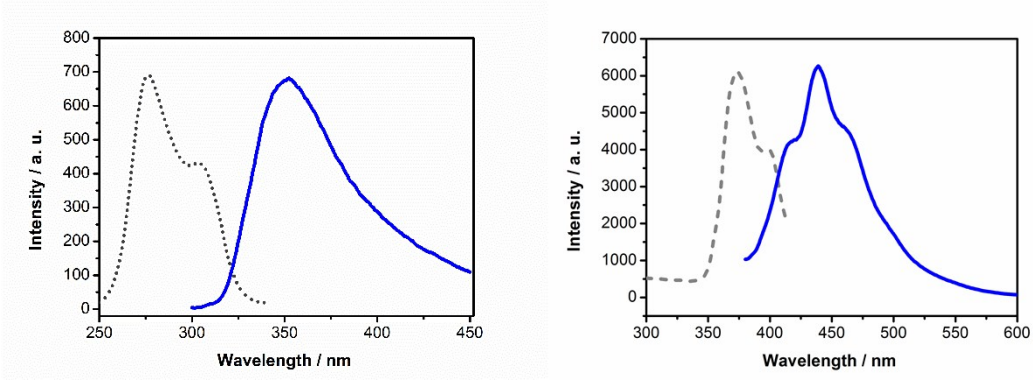

Figure S2. IR spectra of MOF-1 (black solid line), ligands Hbtca (read solid line) and phen (blue solid line).

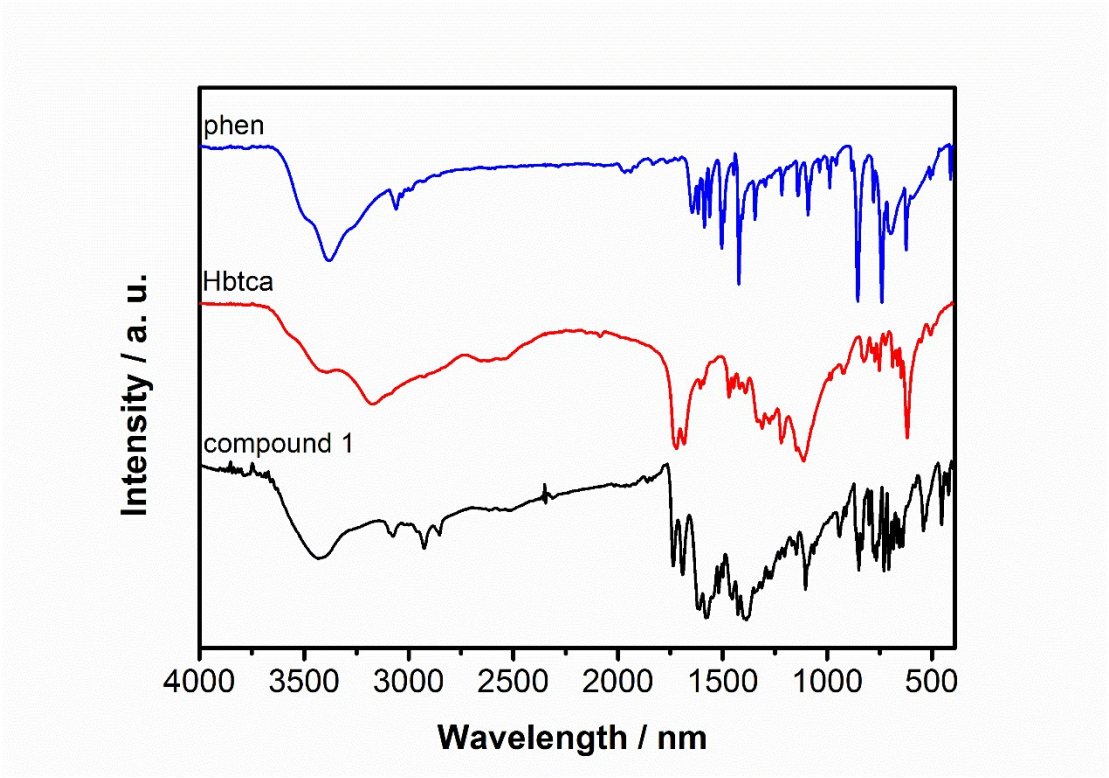

Figure S3. IR spectra of compounds **1–6**.

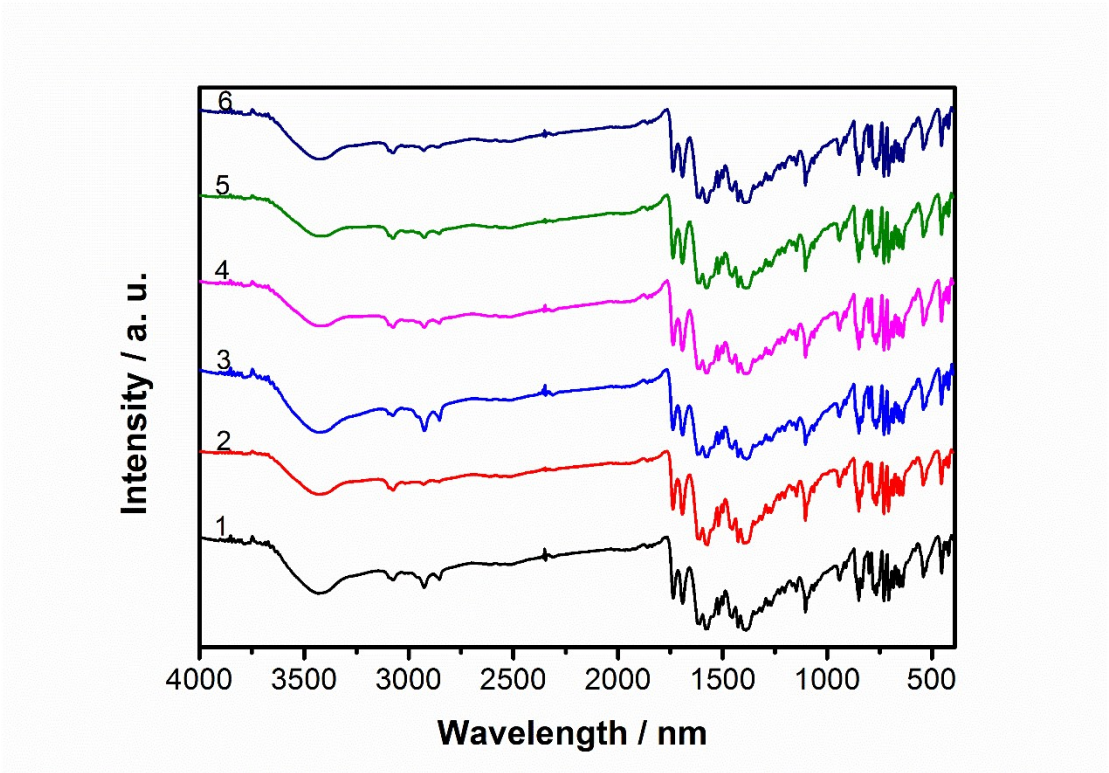

Figure S4. CIE chromaticity diagram (a), emission spectra (b) and the CIE coordinates for [Eu_xTb_{1-x}(Hbtca)(phen)] (**3–6**) upon the excitation at 275 nm.

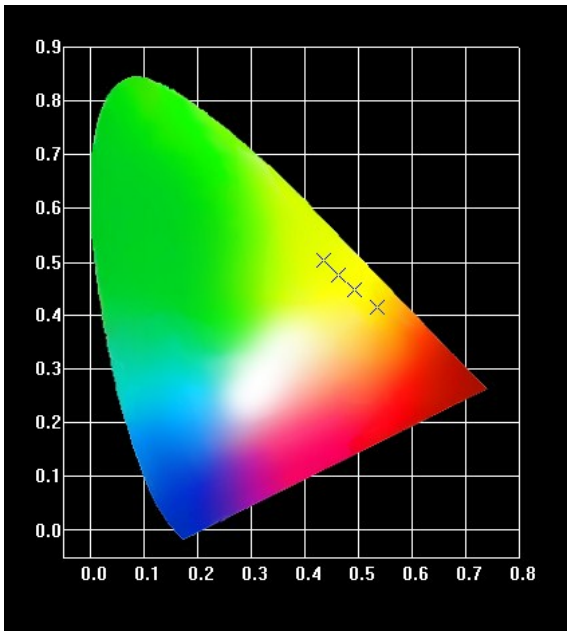

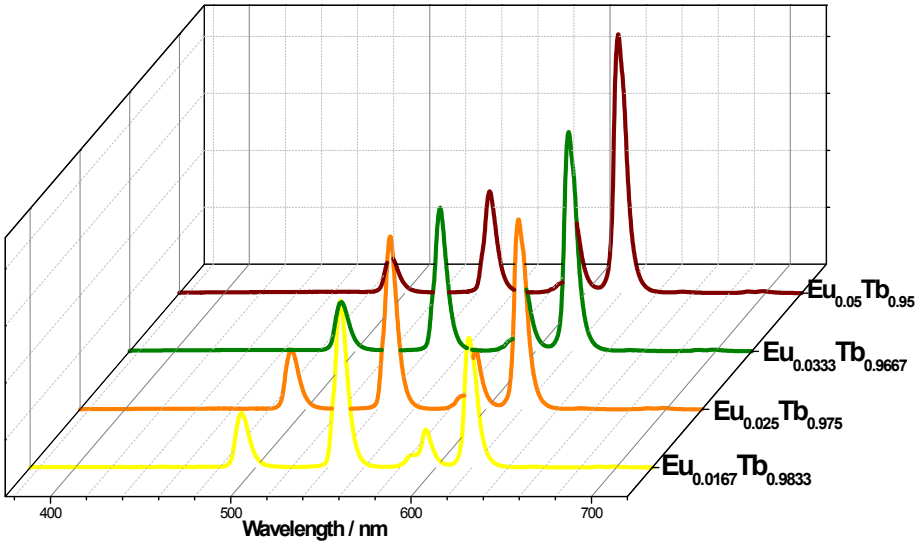

Compound	CIE coordinates λex=275nm
3	(0.436,0.5022)
4	(0.4633,0.4757)
5	(0.4929,0.4483)
6	(0.5351,0.4148)

Figure S5. CIE chromaticity diagram for [Eu_xTb_{1-x}(Hbtca)(phen)] (**3–6**) by change excitation wavelength from 330nm to 365nm and the photo under 365nm xenon lamp. (a) [$Eu_{0.05}Tb_{0.95}$(Hbtca)(phen)], (b) [$Eu_{0.0333}Tb_{0.9667}$(Hbtca)(phen)], (c) [$Eu_{0.025}Tb_{0.975}$(Hbtca)(phen)] and (d) [$Eu_{0.0167}Tb_{0.9833}$(Hbtca)(phen)]

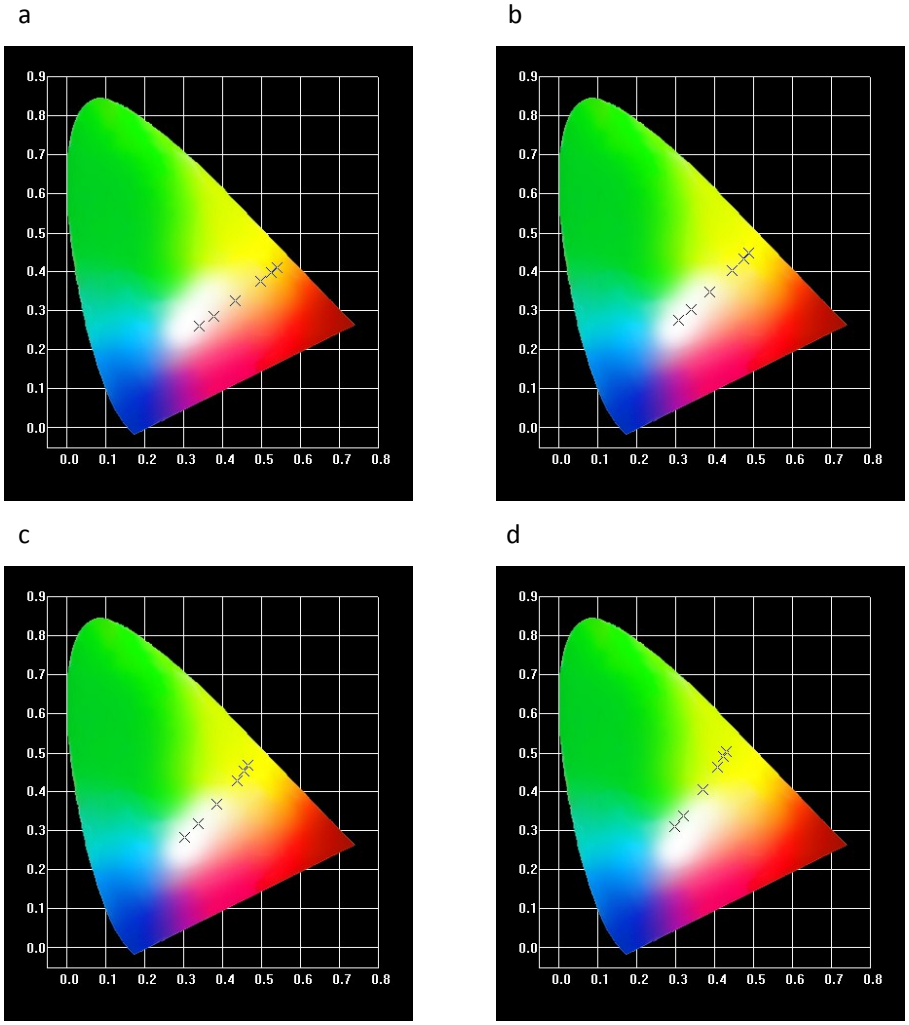

Table S4. The CIE coordinate for [Eu_xTb_{1-x}(Hbtca)(phen)] (**3–6**) by change excitation wavelength from 330nm to 365nm.

	3	**4**	**5**	**6**
330nm	(0.4296,0.5022)	(0.4660,0.4681)	(0.4869,0.4464)	(0.5390,0.4095)
340nm	(0.4220,0.4888)	(0.4560,0.4536)	(0.4762,0.4329)	(0.5247,0.3963)
350nm	(0.4063,0.4636)	(0.4383,0.4268)	(0.4456,0.4036)	(0.4982,0.3744)

355nm	(0.3709,0.4043)	(0.3854,0.3678)	(0.3872,0.3470)	(0.4337,0.3262)
360nm	(0.3199,0.3381)	(0.3377,0.3164)	(0.3409,0.3024)	(0.3779,0.2858)
365nm	(0.2975,0.3111)	(0.3037,0.2833)	(0.3081,0.2753)	(0.3392,0.2607)

Figure S6. The luminescence decay curves for (a) Tb-MOF, (b) Eu-MOF and (c) $Eu_{0.0167}Tb_{0.9833}$–MOF.

a

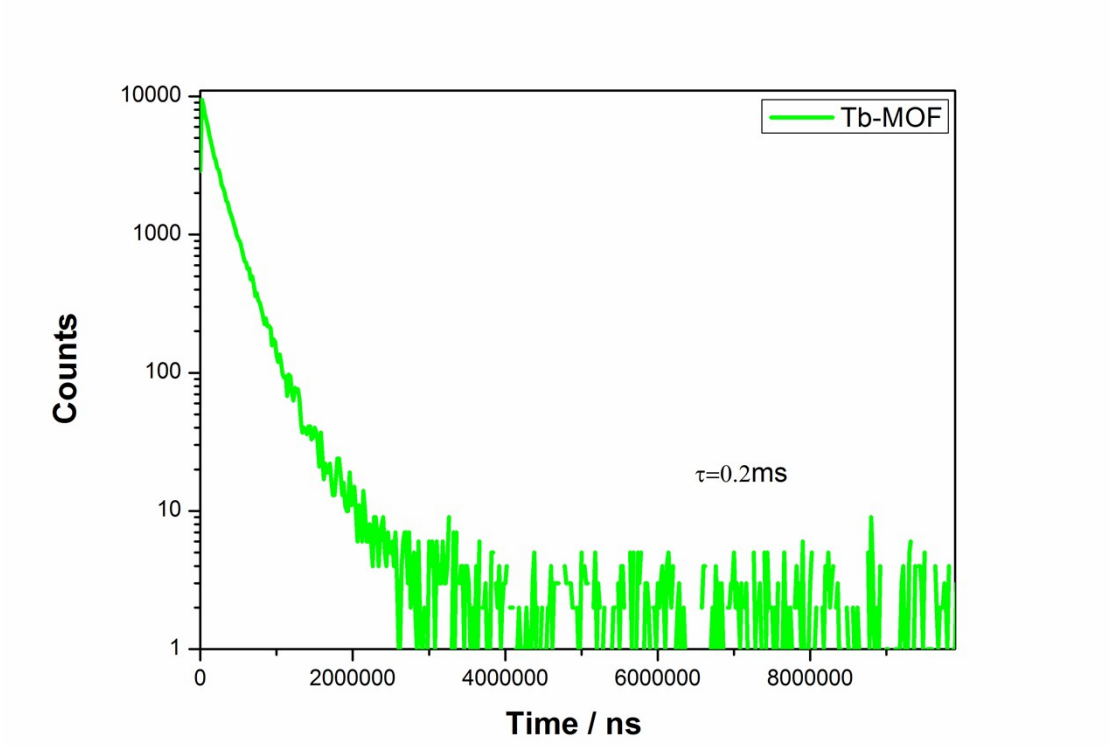

b

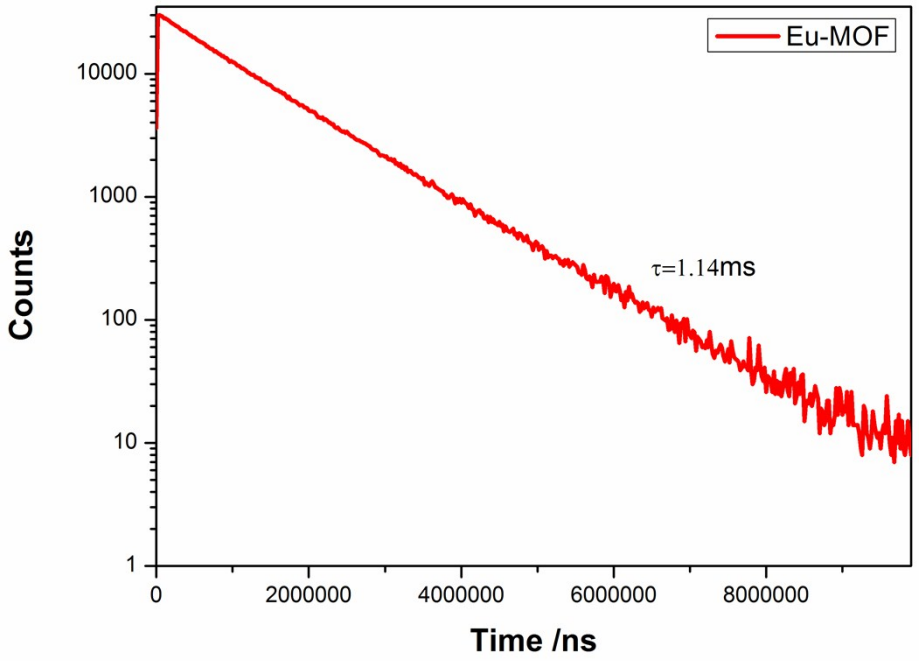
Eu-MOF
τ=1.14ms
Counts
Time /ns
10000
1000
100
10
1
0
2000000
4000000
6000000
8000000

c

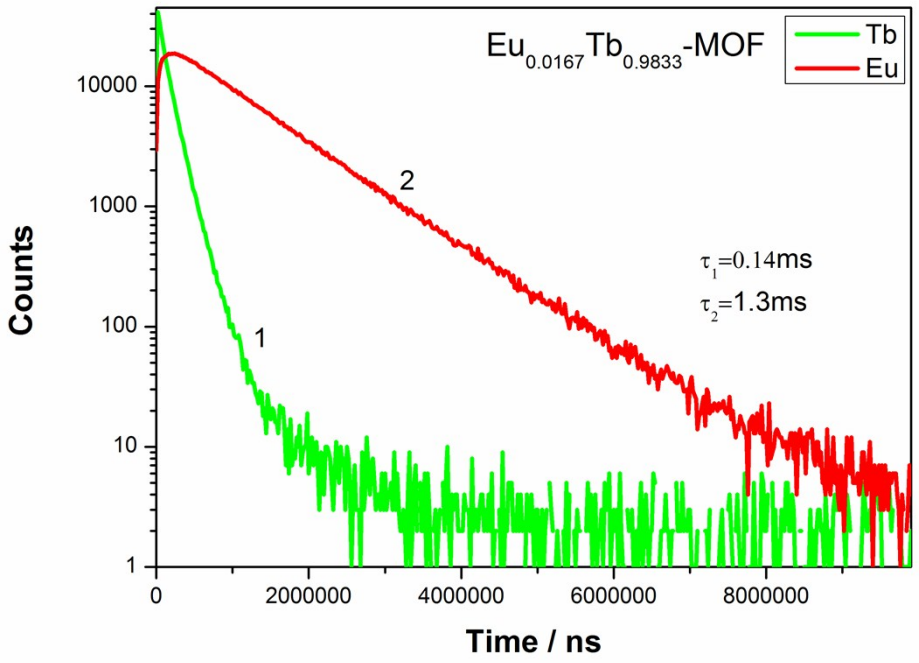
Eu0.0167Tb0.9833-MOF
Tb
Eu
2
1
τ1=0.14ms
τ2=1.3ms
Counts
Time / ns
10000
1000
100
10
1
0
2000000
4000000
6000000
8000000